Geoderma 337 (2019) 384–393

Contents lists available at ScienceDirect

Geoderma

journal homepage: www.elsevier.com/locate/geoderma

Effect of stem basal cover on the sediment transport capacity of overland flows

Hongli Mu[a,b], Xianju Yu[a,b], Suhua Fu[a,b,c,*], Bofu Yu[d], Yingna Liu[a,b], Guanghui Zhang[a,b]

[a] Faculty of Geographical Science, Beijing Normal University, Beijing 100875, PR China
[b] Beijing Key Laboratory of Environmental Remote Sensing and Digital Cities, Beijing Normal University, Beijing 100875, PR China
[c] State Key Laboratory of Soil Erosion and Dryland Farming on the Loess Plateau, Chinese Academy of Sciences and Ministry of Water Resources, Yangling 712100, PR China
[d] Australian Rivers Institute and School of Engineering and Built Environment, Griffith University, Nathan 4111, Australia

ARTICLE INFO

Handling Editor: Yvan Capowiez

Keywords:
Stem basal cover
Sediment transport capacity
Flow discharge
Slope gradient
Overland flow

ABSTRACT

Vegetation cover can effectively prevent soil erosion and plays an important role in soil and water conservation. Accurate estimation of the sediment transport capacity (*Tc*) is critical for soil erosion models. *Tc* data for different levels of vegetation cover, however, are quite limited. The objectives of this study were to evaluate the influence of stem basal cover, slope gradient and discharge on the transport capacity of overland flows for *Tc* prediction. A non-erodible flume (5 m long and 0.37 m wide) was used in this study. The discharge ranged from 0.5×10^{-3} to 2×10^{-3} $m^3 s^{-1}$, the slope gradient was from 8.8% to 25.9% and an artificial stem basal cover of 0, 1.25%, 2.5%, 5%, 10%, 15%, 20%, 25% and 30% was used to represent the natural vegetation. Stems 2 mm in diameter were randomly arranged. The sediment size for the experiment ranged from 0.25 to 0.59 mm with a median diameter of 0.35 mm. The results show that the measured *Tc* decreased exponentially as the stem basal cover increased, and the rate of decrease was far greater than what has been reported in the literature. The transport capacity was affected more by the stem basal cover than by slope and discharge when the cover exceeded approximately 2–3%. The research shows that the surface or stem basal cover plays a critical role in reducing the transport capacity of overland flows.

1. Introduction

Soil erosion is a global issue because of its severe adverse economic and environmental impacts. Soil erosion is defined as the process of detachment and transport of soil material by erosive agents (Ellison, 1947). The rate of soil erosion depends mainly on the detachment of soil particles and the transport capacity of overland runoff (Borrelli, 2013; Julien and Simons, 1985; Lal, 1998). Sediment transport capacity is the maximum sediment load that a flow can carry given particular discharge, slope, surface roughness, and sediment size, among other conditions (Huang et al., 1999; Li and Abrahams, 1999; Zhang et al., 2009). Sediment transport capacity is pivotal to sediment delivery and deposition, and its determination is widely considered and implemented in soil erosion models (De Roo, 1996; Mahmoodabadi et al., 2014a; Nearing et al., 1989; Yu et al., 2015; Zhang et al., 2009).

Many studies of the sediment transport capacity have been undertaken and several equations for calculating the sediment transport capacity of overland flows have been developed (Abrahams et al., 1998; Ali et al., 2012; Finkner et al., 1989; Govers, 1990; Guy et al., 2009; Wu et al., 2018; Zhang et al., 2009). Different experimental materials and methods to measure the transport capacity have been used to simulate natural overland flows. Experimental materials include mainly non-cohesive soil (Ali et al., 2012; Zhang et al., 2009) and cohesive soil (Lei et al., 2001; Mahmoodabadi et al., 2014a). The main methods include non-erodible (Zhang et al., 2009; Zhang et al., 2011b) and erodible bed conditions (Ali et al., 2012; Lei et al., 2001; Mahmoodabadi et al., 2014a). Different hydraulic variables have been used to determine the sediment transport capacity. One of the most frequently used variables is the shear stress (Ali et al., 2012; Finkner et al., 1989; Govers et al., 1992; Zhang et al., 2009). Foster and Meyer (1972) found that the Yalin equation (Yalin, 1963) was suitable to determine the transport capacity of overland flows based on the basic runoff transport capacity equation in the erosion model of Meyer and Wischmeier (1969):

$$\tau = \rho g R S \quad (1)$$

where τ is the shear stress of flow (Pa), ρ is the water mass density ($kg\,m^{-3}$), g is the acceleration due to gravity ($m\,s^{-2}$), S is the slope

* Corresponding author at: Faculty of Geographical Science, Beijing Normal University, Beijing 100875, PR China.
E-mail address: suhua@bnu.edu.cn (S. Fu).

https://doi.org/10.1016/j.geoderma.2018.09.055
Received 16 April 2018; Received in revised form 26 September 2018; Accepted 29 September 2018
0016-7061/ © 2018 Published by Elsevier B.V.

steepness, or the tangent of the slope angle ($m\,m^{-1}$), and R is the hydraulic radius (m). Bagnold (1966) believed that the flow would use available energy to transport the sediment; stream power, or the energy expenditure per unit time, could therefore be an important variable that determines the sediment transport capacity (Bagnold, 1966; Li and Abrahams, 1999; Mahmoodabadi et al., 2014a; Yu et al., 2015; Zhang et al., 2009):

$$\omega = \tau V \quad (2)$$

where ω is the stream power ($kg\,s^{-3}$), V is the mean flow velocity ($m\,s^{-1}$), and τ is the shear stress of flow (Pa). In addition, the effective stream power (Ali et al., 2012; Everaert, 1991; Govers, 1990), unit stream power (Ali et al., 2012; Govers, 1990; Shih and Yang, 2009) and discharge and the slope gradient (Govers and Rauws, 1986; Julien and Simons, 1985; Prosser and Rustomji, 2000; Zhang et al., 2009) are commonly used to represent the flow hydraulics to calculate the transport capacity. Not only different hydraulic variables have been used to predict the transport capacity of overland flows, parameter values to quantify these relationships area also different, mostly because of the different soils and sediments used; of the differences in experiment design, particularly the range of flow rate and slope steepness, and of other conditions that are not well controlled such as surface roughness and soil properties.

Vegetation, which is effective in preventing soil erosion, plays an important role in soil and water conservation (Braud et al., 2001; Pan et al., 2010; Rogers and Schumm, 1991; Zhang et al., 2011a; Zhao et al., 2016). Vegetation effectively reduces rainfall energy and runoff and increases land surface roughness, which decreases flow velocity (Fathi-Maghadam and Kouwen, 1997; Liu et al., 2013; Nanson and Beach, 1977; Wu et al., 2011; Zhang et al., 2018). The results presented by Pan and Shangguan (2006) indicate that the above-ground parts of grasses significantly decreases the sediment yield. The relationship between vegetation cover and soil erosion has been described using both linear and exponential functions (Noble, 1965; Ouyang et al., 2010; Wischmeier, 1959; Zhou et al., 2006). The relationship between vegetation cover and soil erosion under different land-use patterns is shown in Table 1. These studies were conducted mainly under rainfall and using field plots with gentle slopes. The slope gradient was constant for these studies, and the effect of the slope gradient was measured continuously throughout the simulated rainfall event (Pan et al., 2010). An exponential decay function has been extensively used to describe the decrease in soil erosion with vegetation cover for different rainfall intensities (Table 1). Traditional studies of vegetation cover considered the combined effect of leaves and stems, while the separate effect of canopy cover or that of stem basal cover on soil erosion has not been extensively investigated. Zhao et al. (2016) finds that vegetation stems function as the dominant roughness element in overland flow, and they greatly control soil erosion. Soil loss is most severe from cultivated land on steep slopes in China and elsewhere in the world. The land surface in cultivated areas is covered mainly with crop stems. Crop stems can intercept runoff and decrease soil erosion effectively once the overland flow has formed. Thus, vegetation stems may greatly impact the transport capacity of overland flows, especially on cultivated land. However, few studies have examined the effect of vegetation stems on the transport capacity of overland flows.

The objectives of this study are to quantify the effect of vegetation stems on the transport capacity of overland flows for a range of discharge and slope steepness, to better understand the mechanism underlying the role of above-ground vegetation stems in soil and water conservation, and to aid in the design of effective vegetation measures to control soil erosion on steep cropland. In addition, this study provides a complete experimental data set as a reference and such a data set could be used to test and improve the prediction accuracy of soil erosion models.

2. Materials and methods

2.1. Experimental conditions and treatments

This study was conducted at the Fangshan experimental station of Beijing Normal University. The experiments on the sediment transport capacity of overland flows were carried out in a flume (5.0 m long and 0.37 m wide) with a smooth Plexi-glass floor and glass walls (Fig. 1). The bed slope of the flume could be manually adjusted from 0 to 60%. The flume consisted of a 2.4-m-long section covered with vegetation stems and a 2.3-m-long bare section with a layer of sieved sediment, the top 0.3 m was used to house the water tank. To simulate the effect of vegetation stem on the sediment transport capacity of overland flows, Gramineae stems were chosen to ensure that the vegetation stems could protrude through the overland flow. The Gramineae stems all had a diameter of 2 mm and a total height of 12 mm. The stems were artificial and had similar flexibility to those from natural vegetation stems. Moreover, the Gramineae stems can be reused. The basal cover and layout of Gramineae stems can be more easily controlled than those of natural vegetation stem. According to the typical vegetation cover on the Loess Plateau, China, the stem basal cover used in this study was approximately 0, 1.25%, 2.5%, 5%, 10%, 15%, 20%, 25% and 30% and were controlled by the total number of stems and the stem diameter (Table 2). For each level of plant basal cover, a plastic mesh with punched holes was used to secure the artificial Gramineae stems, and the mesh was then placed on the flume bed covered with oil paint. A thick layer of the sieved sand was added into the paint to increase the bed roughness. The stems were glued to the flume bed when the paint was dry, and the bed material for areas not covered with stems was the same as that used for the experiment to measure the sediment transport capacity. The stems were arranged in a random pattern (Fig. 2a), and the stem basal cover of 30% brought about nearly 100% canopy cover (Fig. 2b). The bare 'ground' between the stems (70%) cannot be seen from above the artificial stems because the artificial Gramineae stems are flexible enough to conceal the bare ground surface for a closed canopy.

Sand-laden flow was supplied to the flume to fully simulate overland flow on a natural slope. The sediment, which was collected from the bed of the Yongding River near Beijing, was air dried and first passed through a 2 mm sieve to remove gravel and residues. The sand that passed through 0.59 mm sieve but not 0.25 mm sieve was used as the experimental material. The particle size distributions of the experimental sand are presented in Table 3; the median diameter (d_{50}) was 0.35 mm.

The experimental flume was adjusted to 8.7%, 17.4% and 25.9%, which correspond to the common slope gradient found in the Loess Plateau region. Three discharges were used, i.e., 0.5×10^{-3}, 1.0×10^{-3} and $2.0 \times 10^{-3}\,m^3\,s^{-1}$. These correspond to overland flow from areas of 4 m wide and 9–36 m long with a steady state rainfall intensity of $50\,mm\,h^{-1}$ to contextualize the magnitude of the discharge applied. The discharge was controlled by a series of valves installed in a flow diversion box (Fig. 1). The discharge was collected at the lower end of the flume using plastic buckets and was measured with a volumetric cylinder.

2.2. Experimental measurements

Flow rate, slope gradient and stem basal cover were adjusted to the designated values prior to sediment introduction. The sediment was delivered from a sediment delivery machine that was designed to ensure that the transport capacity was reached for each combination of flow discharge, slope gradient and stem basal cover (Fig. 1). The sediment delivery machine was installed over the flume at a distance of 0.5 m from the top. The sediment feeding rate was controlled by the rotation speed of the rotor and the degree of openness installed within the sediment delivery machine. The sediment feeding rate was adjusted

Table 1
Relationship between vegetation cover and soil erosion rate.

Type of vegetation cover	Equation	Units of soil erosion (E)	Experiment site	Experiment condition	Rainfall intensity	Slope gradient	Reference
Grass, bushes and trees	$E = 0.0668e^{-0.0235C}$	cm y^{-1}	Field	Natural rainfall	–	–	Dunne et al., 1978
	$E = 0.9258e^{-0.0168C}$	–	Field	Natural rainfall	–	–	Rickson and Morgan, 1988
Grasses	$E = 433.43 + 3920.44e^{-0.037C}$, $R^2 = 0.56$	kg ha^{-1}	Plywood boxes	Natural rainfall	468 mm y^{-1}	8.5°	Dadkhah and Gifford, 1980
	$E = 10.4856e^{-0.0300C}$, $R^2 = 0.25$	g m^{-2}	Field plots	Simulated rainfall	33 mm h^{-1}	1–2°	Snelder and Bryan, 1995
	$E = 34.1240e^{-0.0300C}$, $R^2 = 0.37$						
	$E = 653.27e^{-0.0455C}$, $R^2 = 0.62$	g m^{-2}	Field plots	Simulated rainfall	69 mm h^{-1}	–	Moore et al., 1979
	$E = 64.4240e^{-0.0477C}$, $R^2 = 0.99$	t ha^{-1}	Field	Natural rainfall	–	–	Lang, 1990
	$E = 16.857e^{-0.0593C}$, $R^2 = 0.96$						
	$E = 335.38e^{-0.0694C}$, $R^2 = 0.98$						
	$E = 40.480e^{-0.076C}$	t ha^{-1}	Field plots	Simulated rainfall	130 mm h^{-1}	15%	Loch, 2000
Pasture	$E = 0.6667e^{-0.0435C}$	kg ha^{-1}	Field	Natural rainfall	–	4.5%	Elwell and Stocking, 1976
	$E = 0.9559e^{-0.0527C}$		Field plots	Natural rainfall	–	4°	Elwell and Stocking, 1974
	$E = 5.4172e^{-0.0411C}$, $R^2 = 0.99$	g L^{-1}	Field	Simulated rainfall	–	–	Francis and Thornes, 1990
	$E = 5.5669e^{-0.0816C}$, $R^2 = 0.99$						
	$E = 19.072e^{-0.0708C}$, $R^2 = 0.90$	t ha^{-1}	Field plots	Natural rainfall	–	4–8%	Silburn et al., 2011
Rock fragment	$E = 3.638e^{-0.0704C}$, $R^2 = 0.97$	Mg ha^{-1} h^{-1}	Field plots	Simulated rainfall	50 mm h^{-1}; 100 mm h^{-1}; 150 mm h^{-1}	1–5%	Martínez-Zavala and Jordán, 2008
	$E = 38.824e^{-0.0545C}$, $R^2 = 0.98$						
	$E = 125.6e^{-0.0602C}$, $R^2 = 0.96$						
Cultivated land	$E = 136e^{-0.0790C}$, $R^2 = 0.86$	–	Field	Simulated rainfall	65 mm h^{-1}	–	Kainz, 1989
	$E = 765.134e^{-0.0840C}$, $R^2 = 0.37$	g m^{-2}	Field plots	Simulated rainfall	72 mm h^{-1}	0.4–13.8%	Laufer et al., 2016

Note: the equations reflect the combined effect of both above-ground (stems and leaves) and below-ground (roots) biomass. C, vegetation cover (%); E, rate of soil erosion.

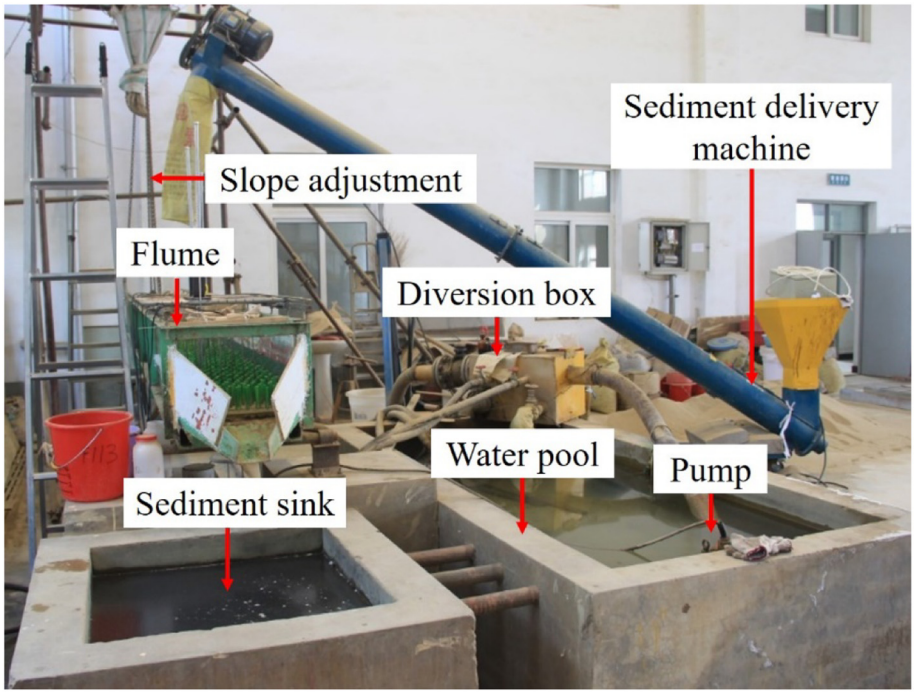

Fig. 1. Experimental setup to measure the sediment transport capacity.

at the beginning of each test and remained fixed during each test. Once the flow velocity and depth were measured, the sediment delivery machine operated until not all of the sediment could be carried and deposition was observed to occur 0.3 m above the outlet, at which point the transport capacity was assumed to have been reached.

Five samples per experiment were collected as quickly as possible using plastic buckets to avoid excessive erosion in the flume. The sampling duration was recorded using a digital stopwatch and was adjusted depending on the flow rate (longer duration for small discharge and shorter duration for higher values) within the range of

Table 2
Nine levels of stem basal cover used in the experiment.

Stem basal cover (%)	0	1.25	2.5	5	10	15	20	25	30
Number of stems	0	3535	7070	14,141	28,280	42,420	56,561	70,701	84,841

3–10 s. The collected samples were allowed to settle for 24 h, and the clear supernatant was decanted from the containers. The remaining wet sediment was oven dried at 105 °C for 24 h. The dry sediment weight was divided by the sampling duration and the flume width to obtain the sediment discharge per unit width. The average sediment discharge in kg m^{-1} s^{-1} of the five samples was used as the representative transport capacity for the given combination of flow rate, slope gradient and stem basal cover (Table 4). The sediment transport capacity was measured for a total of 81 combinations.

2.3. Data analysis

Vegetation stem basal cover was computed by area of stems and flume bed:

$$C = \frac{N\pi D^2}{4WL} \tag{3}$$

where C is the fractional vegetation stem basal cover (−), N is the total number of stems basal over the flume area (Table 2), D is the stem diameter (2×10^{-3} m), W is the flume width (0.37 m), and L is the vegetated length (2.4 m). The unit flow discharge was then computed by dividing the flow discharge by W:

$$q = Q/W \tag{4}$$

where q is the unit discharge (m^2 s^{-1}) and Q is discharge (m^3 s^{-1}). The hydraulic radius (R) was defined as the ratio of the cross-sectional area to the wet perimeter:

$$R = A/P \tag{5}$$

cross-sectional area A (m^2) and wet perimeter P (m) were calculated as follows:

$$A = W*H \tag{6}$$

$$P = 2H + W \tag{7}$$

where H is flow depth (m).

The following statistical indicators were used to evaluate the performance of the transport capacity equations:

i) The absolute mean error, *AME*:

$$AME = \frac{\sum_{i=1}^{n} |(O_i - P_i)|}{n} \tag{8}$$

Table 3
Particle size distribution of the sediment used in the experiment.

Size (mm)	< 0.05	0.05–0.1	0.1–0.25	0.25–0.5	> 0.5
Distribution (%)	0.23	0.36	7.97	69.02	21.73

where O_i the observed, P_i the predicted value, and n the sample size.

ii) The root mean square error, *RMSE:*

$$RMSE = \sqrt{\frac{\sum_{i=1}^{n} (O_i - P_i)^2}{n}} \tag{9}$$

iii) The root mean square error relative to the mean, *RRMSE*:

$$RRMSE = \frac{\sqrt{(1/n)\sum_{i=1}^{n} (O_i - P_i)^2}}{O_m} \tag{10}$$

where O_m is the mean of the observed values.

iv) The Nash–Sutcliffe coefficient of efficiency, *NSE*:

$$NSE = \frac{\sum_{i=1}^{n} (O_i - O_m)^2 - \sum_{i=1}^{n} (P_i - O_i)^2}{\sum_{i=1}^{n} (O_i - O_m)^2} \tag{11}$$

v) The coefficient of determination, R^2:

$$R^2 = \frac{[\sum_{i=1}^{n} (O_i - O_m)(P_i - P_m)]^2}{\sum_{i=1}^{n} (O_i - O_m)^2 \sum_{i=1}^{n} (P_i - P_m)^2} \tag{12}$$

where P_m is the mean of the predicted value.

The sediment transport capacity as a function of the slope gradient, unit flow discharge, and stem basal cover was analysed with nonlinear regression models. The influence of the slope gradient, flow discharge, and stem basal cover on the transport capacity was examined using analysis of variance (*ANOVA*). All analyses were conducted using *SPSS* (Statistical Product and Service Solutions) software (version 20.0) at the 0.05 significance level.

The following sensitivity index was used to evaluate the sensitivity of a parameter:

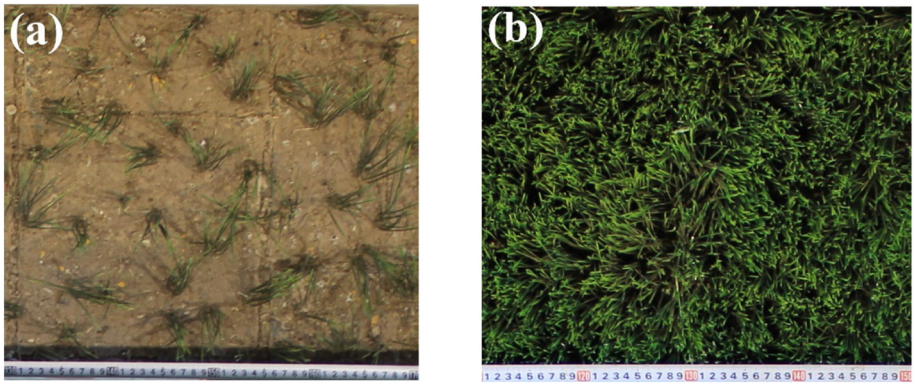

Fig. 2. Arial view of the artificial Gramineae stem basal cover. (a): C = 1.25%, (b): C = 30%.

Table 4
Measured sediment transport capacity (kg m^{-1} s^{-1}) under different combinations of stem basal cover, flow discharge and slope gradient.

Slope gradient (m m^{-1})	Flow discharge (10^{-3} m^3 s^{-1})	Stem basal cover (%)								
		0	1.25	2.5	5	10	15	20	25	30
8.8	0.5	0.104	0.069	0.032	0.018	0.009	0.000	0.000	0.000	0.000
	1.0	0.260	0.140	0.061	0.030	0.019	0.006	0.000	0.000	0.000
	2.0	0.744	0.315	0.141	0.050	0.026	0.008	0.000	0.000	0.000
17.4	0.5	0.556	0.481	0.211	0.158	0.066	0.041	0.022	0.014	0.000
	1.0	1.421	0.863	0.313	0.216	0.106	0.055	0.030	0.019	0.000
	2.0	3.545	1.759	0.707	0.471	0.171	0.083	0.044	0.032	0.018
25.9	0.5	1.315	0.892	0.747	0.425	0.197	0.121	0.072	0.063	0.043
	1.0	3.024	1.918	1.057	0.649	0.319	0.163	0.111	0.097	0.097
	2.0	5.032	3.208	2.024	1.276	0.475	0.305	0.214	0.105	0.130

$$Sen = \left| \frac{(y - y_0)/y_0}{(x - x_0)/x_0} \right| \quad (13)$$

where x_0 is the calibrated parameter value, and x is an adjusted parameter value and was changed by ± 10% based on the x_0 value. The change in the parameter value ($\Delta x = x–x_0$) led to a variation in model output from y_0 to y. The ratio of Δy (i.e., $y–y_0$) to Δx is an approximation of the partial derivative of the model output with respect to the model parameters, and is commonly used as a straightforward measure of model sensitivity (Saltelli et al., 2004). In this study, the ratio of $\Delta y/y_0$ to $\Delta x/x_0$ was used as a measure of the relative sensitivity of predicted sediment transport capacity to stem basal cover, slope gradient and discharge. The relationship between transport capacity (Tc) and stem basal cover (C), slope gradient (S) and unit flow discharge (q) was assumed to follows:

$$Tc = aS^b q^m e^{-kC} \quad (14)$$

where a and k are constants, b and m are the exponent of slope (S) and unit discharge (q), respectively. It is mathematically trivial to show that the sensitivity index so defined is the exponent b with respect to S, and m with respect to q. This implies that the sensitivity index for Tc in relation to slope and discharge is constant, and does not vary with S and q. On the other hand, the sensitivity index with respect to stem basal cover (C) is $-kC$.

3. Results

3.1. Sediment transport capacity with no basal cover

The measured sediment transport capacity (Tc) ranged from 0.104 to 5.032 kg m^{-1} s^{-1} for 0 stem basal cover. Tc was significantly affected by discharge and slope gradient ($p < 0.01$) and increased with the increasing discharge and slope gradient (Table 4). Nonlinear regression analysis between sediment transport capacity and unit discharge and slope gradient when $C = 0$ were carried out and Eq. (15) was obtained:

$$Tc_0 = 6657.972S^{1.493}q^{0.979} \quad R^2 = 0.97 \quad NSE = 0.96 \quad (15)$$

where Tc_0 is the transport capacity for 0 stem basal cover (kg m^{-1} s^{-1}), S is the slope gradient (m m^{-1}), and q is the unit discharge (m^2 s^{-1}). Eq. (15) fitted the measured transport capacity quite well with an R^2 value of 0.97, NSE of 0.96, AME of 0.06 kg m^{-1} s^{-1}, $RMSE$ of 0.30 kg m^{-1} s^{-1} and $RRMSE$ of 0.17 (Table 5, Fig. 3). Similarly, the sediment transport capacity can be expressed as a function of the stream power when $C = 0$:

$$Tc_0 = 0.166\omega_0^{1.336} \quad R^2 = 0.95 \quad NSE = 0.95 \quad (16)$$

where ω_0 is stream power for 0 stem basal cover (kg s^{-3}). The measured Tc was well predicted by the stream power, with an R^2 value of 0.95, NSE of 0.95, AME of 0.05 kg m^{-1} s^{-1}, $RMSE$ of 0.37 kg m^{-1} s^{-1} and $RRMSE$ of 0.21 (Table 6).

3.2. Effect of stem basal cover on sediment transport capacity

The measured sediment transport capacity (Tc) ranged from 0.000 to 3.208 kg m^{-1} s^{-1} for stem basal cover > 0 (Table 4). The stem basal cover of 1.25–30% resulted in a decrease of 45–99% in Tc compared with Tc_0. Tc was a power function of the stem basal cover for each combination of the slope gradient and discharge with the R^2 value ranging from 0.96 to 0.98. The transport capacity decreased rapidly in the presence of vegetation stems in the flume, especially when the stem basal cover exceeded 5% (Fig. 4). The sediment could not be transported when the stem basal cover exceeded 20% and the slope was 8.8%. To evaluate the effect of stem basal covers on the transport capacity, the transport capacity under different stem basal cover was normalized to eliminate the effect of the slope gradient and discharge. The relative sediment transport capacity (R_T) under different stem basal covers were calculated using Eq. (17) for the same combination of a slope gradient and discharge.

$$R_T = Tc/Tc_0 \quad (17)$$

where Tc and Tc_0 represent the transport capacity at a given stem basal cover and at 0 stem basal cover, respectively, and Tc_0 was calculated using Eq. (15). R_T equals 1 when $C = 0$, and $R_T < 1$ when $C > 0$. R_T decreases with the stem basal cover as shown in Fig. 5. R_T decreases sharply when the stem basal cover is < 10% and then decreases slowly when the stem basal cover exceeds 10% (Fig. 5). An exponential relationship was developed between R_T and stem basal cover.

$$R_T = \exp(-0.495C) \quad R^2 = 0.92 \quad (18)$$

where C is the stem basal cover (%). Combining Eq. (17) and Eq. (18) leads to the following equation for the sediment transport capacity for all 81 slope-discharge-cover combinations:

$$Tc = Tc_0^* \exp(-0.495C) \quad R^2 = 0.92 \quad NSE = 0.86 \quad (19)$$

Eq. (19) adequately predicts the measured transport capacity (Fig. 6), with an R^2 value of 0.92, NSE of 0.86, AME of 0.07 kg m^{-1} s^{-1} and $RMSE$ of 0.21 kg m^{-1} s^{-1}.

3.3. The effect of stem basal cover, slope gradient and discharge on sediment transport capacity

The measured sediment transport capacity for different stem basal cover, slope gradient, and flow discharge are presented in Table 4. The minimum transport capacity was 0 kg m^{-1} s^{-1} because the overland flow could not transport any sediment under a high stem basal cover and a gentle slope. The measured transport capacity decreased with the increasing stem basal cover and increased as the discharge and slope gradient increased (Fig. 4). The transport capacity was greatly affected by the stem basal cover, slope and discharge ($P < 0.01$). Sensitivity analysis based on the first order difference was used to indicate the relative importance of each of the three factors, namely the stem basal cover, slope, and discharge. The relative change in the transport

Table 5
Performance of various empirical equations for the sediment transport capacity (kg m^{-1} s^{-1}) under independent variables of slope and discharge without cover.

Reference	Equation	Flume scale (m^2)	Slope (m m^{-1})	Unit discharge (10^{-3} m^2 s^{-1})	Experiment condition	Experiment material	d_{50} or *MWD* (mm)	*AME* (kg m^{-1} s^{-1})	*RMSE* (kg m^{-1} s^{-1})	*RRMSE*	*NSE*	R^2
Ali et al., 2012	$Tc = 0.17 \times 10^6 Q^{1.46} S^{2.89} / d_{50}^{0.5}$	3 × 0.5	5.2–17.6	0.07–2.07	Eroding bed	Sand	0.233, 0.536, 0.719, 1.022	2.97	5.67	3.19	−11.44	0.87
Mahmoodabadi et al., 2014a	$Tc = 8590.1 q^{0.855} S^{1.872}$	6 × 1.0	2–6	–	Eroding bed	Soil	0.77 0.33 0.19	0.84	1.17	0.66	0.47	0.94
Zhang et al., 2011b	$Tc = 2382.32 q^{1.269} S^{1.637} d_{50}^{-0.345}$	5 × 0.4	8.8–46.6	0.66–5.26	Non-eroding bed	Sand	0.10 0.22 0.41 0.69 1.16	0.17	0.42	0.23	0.93	0.94
This study	$Tc_0 = 6657.972 q^{0.979} S^{1.493}$	5 × 0.37	8.8–25.9	1.35–5.41	Non-eroding bed	Sand	0.35	0.06	0.30	0.17	0.97	0.97

Note: Q, the total discharge in flume (m^3 s^{-1}); q, unit discharge (m^2 s^{-1}); S, slope (mm^{-1}); d_{50}, the median diameter (mm); *MWD*, mean weigh diameter (mm); *AME*, absolute mean error (kg m^{-1} s^{-1}); *RMSE*, root of the mean squared error (kg m^{-1} s^{-1}); *RRMSE*, relative root mean square error; *NSE*, Nash-Sutcliffe efficiency coefficient; R^2, coefficient of determination.

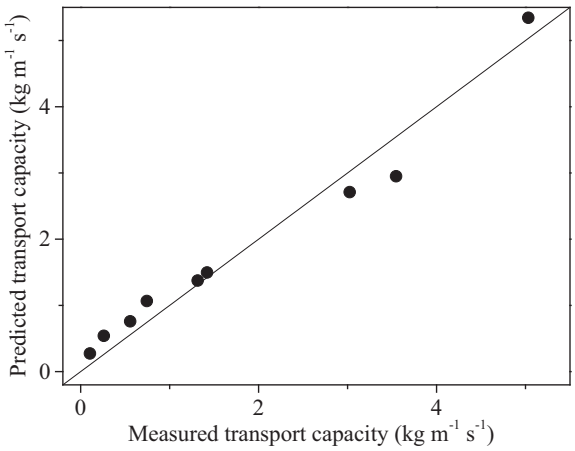

Fig. 3. Comparison between measured and predicted (using Eq. (15)) transport capacity.

capacity for given relative changes in these factors can be written as follows:

$$\frac{\Delta T_C S}{T_C \Delta S} = 1.493 \tag{20}$$

$$\frac{\Delta T_C q}{T_C \Delta q} = 0.979 \tag{21}$$

$$\frac{\Delta T_C C}{T_C \Delta C} = -0.495C \tag{22}$$

For given relative change in the slope and unit discharge, the relative change in the transport capacity is constant (Eqs. (20), (21)). The sediment transport capacity is more sensitive to the slope gradient than to discharge. For the stem basal cover, the relative change in the transport capacity for a given relative change in stem basal cover is a linear function of the stem basal cover (Eq. (22)). The higher the level of cover, the more sensitive the transport capacity is to change in the cover in relative terms. The sensitivity analysis results show that when the stem basal cover exceeds approximately 2%, the effect of stem basal cover will be greater than that of discharge on the transport capacity, and when the stem basal cover is more than about 3%, the effect of the stem basal cover is greater than that of slope gradient. This comparison based on sensitivity analysis indicates that the vegetation cover affects the sediment transport greatly, especially when the level of cover is high.

4. Discussion

4.1. Performance of equations on sediment transport capacity with no basal cover

There were numerous studies of the sediment transport capacity without basal cover (Abrahams et al., 1998; Ali et al., 2012; Prosser and Rustomji, 2000; Govers, 1990; Lei et al., 2001; Mahmoodabadi et al., 2014a; Mahmoodabadi et al., 2014b; Wu et al., 2018; Zhang et al., 2011a, 2011b). However, the experiment results showed some differences because of the different experimental conditions and different materials used. It is of importance that the experiment data are as accurate and experiment results are as reproducible as possible. Since the experimental method for this study was the same as that in Zhang et al. (2011b) and similar sediments in terms of the particle size were used in both experiments, the predicted transport capacity of this study was compared with the *Tc* predicted by Zhang et al. (2011b). The predicted *Tc* values using the equations from Zhang et al. (2011b), especially the one for a median diameter of 0.41 mm, were close to that from Eq. (16) in this study for the same value of stream power (Fig. 7). The median

Table 6
Performance of various empirical equations for the sediment transport capacity ($kg\,m^{-1}\,s^{-1}$) under independent variables of stream power without cover.

Reference	Equation	d_{50} (mm)	Flume scale (m^2)	Slope ($m\,m^{-1}$)	Unit discharge ($10^{-3}\,m^2\,s^{-1}$)	Experiment condition	Experiment material	*AME* ($kg\,m^{-1}\,s^{-1}$)	*RMSE* ($kg\,m^{-1}\,s^{-1}$)	*RRMSE*	*NSE*	R^2
Zhang et al., 2011b	$Tc = 0.238\omega^{1.266}$	0.10	5 × 0.4	8.8–46.6	0.66–5.26	Non-eroding bed	Sand	0.50	0.64	0.36	0.84	0.95
	$Tc = 0.178\omega^{1.413}$	0.22						0.52	0.76	0.43	0.78	0.94
	$Tc = 0.141\omega^{1.423}$	0.41						0.08	0.39	0.22	0.94	0.94
	$Tc = 0.117\omega^{1.435}$	0.69						0.20	0.47	0.26	0.91	0.94
	$Tc = 0.095\omega^{1.441}$	1.16						0.48	0.75	0.42	0.78	0.94
This study	$Tc_0 = 0.166\omega_0^{1.336}$	0.35	5 × 0.37	8.8–25.9	1.35–5.41	Non-eroding bed	Sand	0.05	0.37	0.21	0.95	0.95

Note: *Tc*, sediment transport capacity ($kg\,m^{-1}\,s^{-1}$); ω, stream power ($kg\,s^{-3}$); d_{50}, the median diameter (mm); *AME*, absolute mean error ($kg\,m^{-1}\,s^{-1}$); *RMSE*, root of the mean squared error ($kg\,m^{-1}\,s^{-1}$); *RRMSE*, relative root mean square error; *NSE*, Nash-Sutcliffe efficiency coefficient; R^2, coefficient of determination.

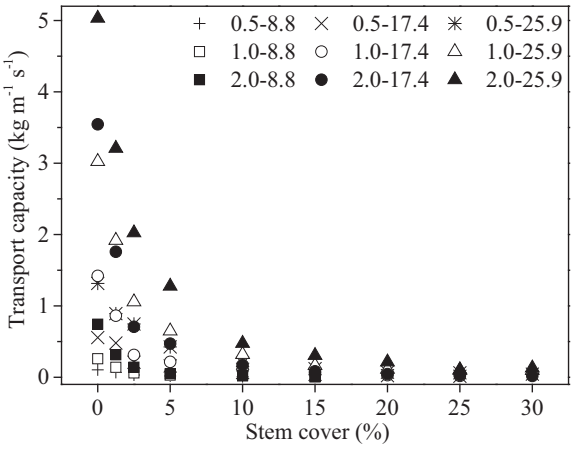

Fig. 4. Transport capacity (*Tc*) for different stem basal covers. Flow discharge: 0.5, 1.0, 2.0 ($10^{-3}\,m^3\,s^{-1}$); slope gradient: 8.8, 17.4, and 25.9%.

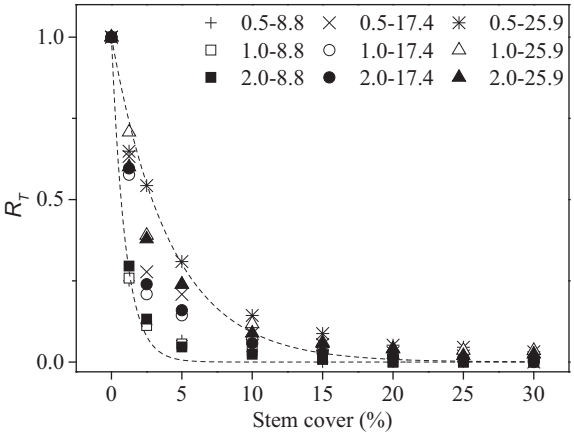

Fig. 5. Relation of R_T and stem basal cover (*C*). The dotted lines were upper and under included line; flow discharge: 0.5, 1.0, and 2.0 ($*10^{-3}\,m^3\,s^{-1}$); slope gradient: 8.8, 17.4, and 25.9%.

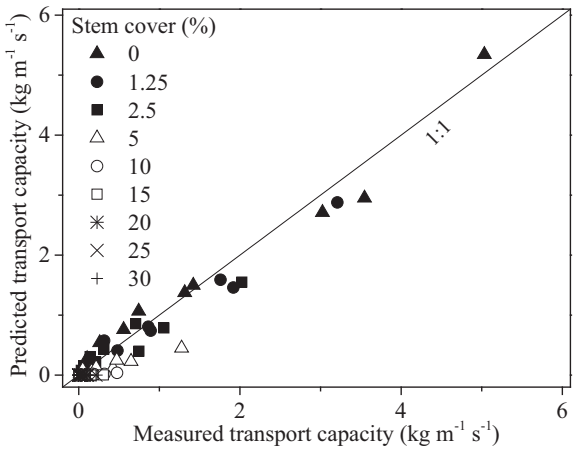

Fig. 6. Comparison between measured and predicted (using Eq. (19)) transport capacity.

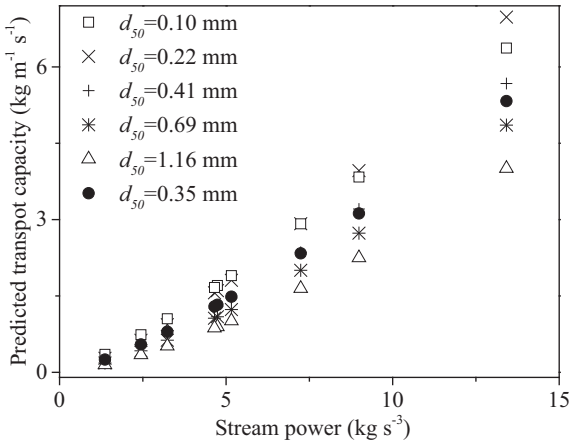

Fig. 7. Comparison predicted *Tc* by equations between this study and Zhang et al. (2011b) for the same level of stream power. These equations of d_{50} = 0.10, 0.22 0.41, 0.69, 1.16 mm were from Zhang et al. (2011b) and the equation of d_{50} = 0.35 mm was from this study.

particle size affected the relationship between the sediment transport capacity and stream power. This resulted in the differences in the exponent for stream power for different median diameters, it does coincide with that provided by Mahmoodabadi et al. (2014b). Table 6 shows the performance of the equations compared with the measured transport capacity in this study. The results show that the equation for sediments with a median diameter of 0.41 mm has the same level of accuracy as Eq. (16) with a median diameter of 0.35 mm from this study. The *NSE* values were 0.94 and 0.95, and the *RMSE* were 0.39 and 0.37 for a median diameter of 0.41 mm and 0.35 mm, respectively (Table 6). These results indicate that the experimental methods and data of this study and those of Zhang et al. (2011b) are consistent and reproducible.

The sediment transport capacity could be predicted by a power function (Eq. (15)) of the unit discharge, and slope gradient when $C = 0$. The exponent values for the unit flow discharge and slope gradient in this study were 0.979 and 1.493, respectively, and were in the range between 0.82 and 2.0 reported by Prosser and Rustomji (2000). Table 5 shows that the equation from Zhang et al. (2011b), developed with non-eroding beds, provided higher *NSE*, and R^2 and lower *RMSE*, which were close to those from Eq. (15) in this study. This finding

indicates that similar experimental conditions provided similar results. However, the equations from Ali et al. (2012) and Mahmoodabadi et al. (2014a), developed with eroding beds, resulted in lower *NSE* values (Table 5). This finding implies that the transport capacity equation obtained using an eroding bed was not compatible with the current study. The possible reason is that micro-rills could form on an eroding bed, which would increase the surface roughness and alter the hydraulic conditions. In addition, Table 5 shows that the exponent for the slope is greater than that for the unit discharge from this and other studies. This finding indicates that the slope plays a more important role in determining sediment transport capacity than discharge when $C = 0$.

4.2. Comparison of the relationship between vegetation cover and sediment transport capacity

Soil surface conditions such as vegetation and rock fragment cover greatly affect runoff generation and erosion (Papy and Douyer, 1991; Auzet et al., 1995). Soil loss is reduced as the vegetation cover is increased (Benito et al., 2003; Pan and Shangguan, 2006). In this study, the measured transport capacity also decreased with the increasing stem basal cover. However our results are different from those presented by Bunte and Poesen (1993), who showed that the sediment yield increased with the rock fragment cover up to approximately 20% and then decreased as the percent cover exceeded 20%. The different results could be caused by the different experimental methods. In the experiments of Bunte and Poesen (1993), a highly erodible sediment surface covered by rock fragments was used and scour holes could develop to their full extent when rock fragment cover varied from 0 to 20%. Strong local turbulence was created and the sediment yield increased. For rock fragment cover > 20%, the development of scour holes was hampered by limited space between rock fragments, which resulted in a decrease in the sediment yield with increasing rock fragment cover. In this study, non-erodible bed was used and the stem basal cover effectively increased the roughness, reduced the flow energy and consequently decreased the sediment transport capacity and sediment yield.

The sediment transport capacity decreased as an exponential function of stem basal cover, and the coefficient for this experiment was 0.495, whereas the coefficient from other studies reported in Table 1 was all < 0.1 using different vegetation cover types. To further compare the differences in the cover effect on soil erosion and sediment transport capacity, the relative reduction in the soil erosion or the transport capacity from this study (R_C) was calculated using Eq. (23) for specific covers of 2.5%, 10%, and 30%:

$$R_C = \frac{E_C}{E_0} \tag{23}$$

where E_C is the amount of soil erosion or the transport capacity for different levels of vegetation cover, and E_0 is the corresponding soil erosion or the transport capacity without vegetation cover ($C = 0$). Then, the average R_C (Ac), was calculated for each vegetation cover type:

$$A_C = \frac{1}{n}\sum^{n} R_C \tag{24}$$

where n is the number of Rc values for the same cover type, ranging from 8 for grasses (*Gr*) to 2 for grass, bushes and trees (*GBT*) and cultivated land (Table 1).

The reduction factor (A_C) for areas consisting of grass, bushes and trees (*GBT*) was the largest (Table 7), and this is larger than that for grass (*Gr*), pasture (*Pa*), rock fragments (*Ro*) and cultivated land (*CL*) in that order. The reduction factor for stem basal cover was the smallest. The differences in the reduction factor occurred may be because of the way that cover was defined. For the reduction factor of *GBT, Gr, Pa* and *CL*, canopy cover was used to represent the vegetation cover, while the stem basal cover was used in this study. The canopy cover is generally greater than the plant basal cover. Under the same cover percentage, plant stem provides higher surface roughness which decrease flow velocity and the sediment transport capacity. Stem basal cover plays a more important role in reducing the sediment transport capacity and soil erosion. In addition, different soil particle size was used. The sand (d_{50} = 0.35 mm) used in this study was much coarser than those in other experiments reported in the literature (Table 7). Zhang et al. (2011b) also indicated that the transport capacity increases as the soil particle size decreases. Meanwhile, *GBT* had a thicker stem near the surface, so the stem diameter may be another factor to have affected soil erosion. The bed form was also different. The stem basal cover and rock fragments cover were both on the surface, but the reduction factor values for stem basal cover were still smaller than that for rock fragments cover. The main difference was an erodible bed with rock fragments (Bunte and Poesen, 1993) and a non-erodible bed with uniform sand for this study.

The reduction factor for stem basal cover was close to those for *GBT*, *Gr*, *Pa*, *Ro,* and *CL* from reported in the literature when the stem basal cover was < 2.5% (Table 7), and the difference in the reduction factor was quite obvious when the stem basal cover was > 10%. The difference increases as the level of cover increases. This finding indicated that the stem basal cover had a greater effect on the transport capacity than other vegetation types especially when the cover was high.

Compared to artificial stem basal cover of this research, there were quite a few other studies on soil erosion under natural vegetation cover (Benito et al., 2003; Dunne et al., 1978; Elwell and Stocking, 1976; Francis and Thornes, 1990; Loch, 2000; Pan and Shangguan, 2006; Snelder and Bryan, 1995), but the research of natural vegetation cover on sediment transport capacity as distinct from soil erosion was quite limited. Thus the difference between the artificial stem basal cover and the natural vegetation cover on sediment transport capacity is worthy of further investigation because of the limitation of this study in using artificial stem basal cover for this set of experiments.

5. Conclusions

The following conclusions are reached based on this experimental study of the effect of stem basal cover on the sediment transport capacity:

- The relationship between the stream power and transport capacity based on a previous experiment without vegetation cover was confirmed, supporting the experimental methodology and data quality used for this experiment.
- For the sediment used in this experiment, the transport capacity decreases exponentially with the stem cover, and the transport capacity would be reduced to zero when the stem basal cover exceeded 20% and the slope was no > 8.8%. The coefficient of the exponential function was significantly different from those reported in the literature for other cover types, and the difference is most noticeable when the stem basal cover is large. Vegetation cover near the surface or stem basal cover plays a significant role in reducing the transport capacity of overland flows.
- Compared to the slope and flow rate, this study shows that the sediment transport capacity is most sensitive to the stem basal cover when the cover is > 2–3% based on this experiment. This finding implies that surface or stem basal cover should be considered as an effective means of reducing the transport capacity of overland flows for soil conservation.

Acknowledgements

The research described in this paper was funded by the State Key Program of the National Natural Science Foundation of China (No. 41530858), the National Natural Science Foundation of China (No.

Table 7
Erosion reduction factor (*Ac*) for different vegetation cover types.

Vegetation cover type	$A_{2.5}$	A_{10}	A_{30}	References
Grass, bushes and trees	0.9509	0.8180	0.5491	Dunne et al., 1978; Rickson and Morgan, 1988
Grasses	0.8797	0.6053	0.2419	Dadkhah and Gifford, 1980; Snelder and Bryan, 1995; Moore et al., 1979; Lang, 1990; Loch, 2000
Pasture	0.8658	0.5671	0.1949	Elwell and Stocking, 1974, 1976; Francis and Thornes, 1990; Silburn et al., 2011
Rock fragment	0.8572	0.5407	0.1601	Martínez-Zavala and Jordán, 2008
Cultivated land	0.8157	0.4428	0.0870	Kainz, 1989; Laufer et al., 2016
Stem basal cover	0.2901	0.0071	< 0.0001	This study

Note: A_C was the average reduction in the rate of erosion (*Rc*), i.e. E_C over E_0; where E_0 is the soil erosion amount or transport capacity when cover was 0%; E_C the soil erosion amount or transport capacity with different level of vegetation cover.

41571259), the CAS "Light of West China" program, the program for Changjiang Scholars and Innovative Research Team in University, the open project fund from the State Key Laboratory of Soil Erosion and Dryland Farming on Loess Plateau (A314021402-1601) and the China Scholarship Council.

References

Abrahams, A.D., Li, G., Krishnan, C., Atkinson, J.F., 1998. Predicting sediment transport by interrill overland flow on rough surfaces. Earth Surf. Process. Landf. 23, 1087–1099.

Ali, M., Sterk, G., Seeger, M., Boersema, M., Peters, P., 2012. Effect of hydraulic parameters on sediment transport capacity in overland flow over erodible beds. Hydrol. Earth Syst. Sci. 16, 591–601.

Auzet, A.V., Boiffin, J., Ludwig, B., 1995. Concentrated flow erosion in cultivated catchments: influence of soil surface state. Earth Surf. Process. Landf. 20, 5–14.

Bagnold, R.A., 1966. An Approach to the Sediment Transport Problem from General Physics, General Physics Geological Survey. United States Government Printing Office, Washington.

Benito, E., Santiago, J., De Blas, E., Varela, M., 2003. Deforestation of water-repellent soils in Galicia (NW Spain): effects on surface runoff and erosion under simulated rainfall. Earth Surf. Process. Landf. 28, 145–155.

Borrelli, P., 2013. Modelling post-tree-harvesting soil erosion and sediment deposition potential in the Turano River Basin (Italian Central Apennine). Land Degrad. Dev. 26, 356–366.

Braud, I., Vich, A.I.J., Zuluaga, J., Fornero, L., Pedrani, A., 2001. Vegetation influence on runoff and sediment yield in the Andes region: observation and modelling. J. Hydrol. 254, 124–144.

Bunte, K., Poesen, J., 1993. Effects of rock fragment covers on erosion and transport of noncohesive sediment by shallow overland flow. Water Resour. Res. 29, 1415–1424.

Dadkhah, M., Gifford, G.F., 1980. Influence of vegetation, rock cover and trampling on infiltration rates and sediment production. Jam. Water Resour. As. 16, 979–986.

De Roo, A.P.J., 1996. LISEM: a single-event physically based hydrological and soil erosion model for drainage basins. I: theory, input and output. Hydrol. Process. 10, 1107–1117.

Dunne, T., Dietrich, W.E., Brunengo, M.J., 1978. Recent and past erosion rates in semi-arid Kenya. Z. Geomorphol. Suppl. Bd. 29, 130–140.

Ellison, W.D., 1947. Soil erosion studies - Part I. Agric. Eng. 28, 145–146.

Elwell, H.A., Stocking, M.A., 1974. Rainfall parameters and a cover model to predict runoff and soil loss from grazing trials in the Rhodesian sandveld. Proc. Grassld. Soc. Sth. Afr. 9, 157–164.

Elwell, H.A., Stocking, M.A., 1976. Vegetal cover to estimate soil erosion hazard in Rhodesia. Geoderma 15, 61–70.

Everaert, W., 1991. Empirical relations for the sediment transport capacity of interrill flow. Earth Surf. Process. Landf. 16, 513–532.

Fathi-Maghadam, M., Kouwen, N., 1997. Nonrigid, nonsubmerged, vegetative roughness on floodplains. J. Hydraul. Eng. 123, 51–57.

Finkner, S.C., Nearing, M.A., Foster, G.R., Gilley, J.E., 1989. Simplified equation for modeling sediment transport capacity. Trans. ASAE 32, 1545–1550.

Foster, G.R., Meyer, L.D., 1972. Transport of soil particles by shallow flow. Trans. ASAE 51, 99–102.

Francis, C.F., Thornes, J.B., 1990. Runoff hydrographs from three Mediterranean vegetation cover types. In: Thornes, J.B. (Ed.), Vegetation and Erosion, Processes and Environments. Wiley, Chichester, pp. 363–384.

Govers, G., 1990. Empirical relationships for the transport capacity of overland flow. In: Erosion, Transport, and Deposition Processes, Proceedings of Jerusalem Workshop. Jerusalem, Israel, pp. 45–63.

Govers, G., Rauws, G., 1986. Transporting capacity of overland flow on plane and on irregular beds. Earth Surf. Process. Landf. 11, 515–524.

Govers, G., Parsons, A.J., Abrahams, A.D., 1992. Evaluation of transporting capacity formulae for overland flow conditions. In: Parsons, A.J., Abrahams, A.D. (Eds.), Overland Flow Hydraulics and Erosion Mechanics. University College London Press, London (PP).

Guy, B.T., Rudra, R.P., Dickenson, W.T., Sohrabi, T.M., 2009. Empirical model for calculating sediment-transport capacity in shallow overland flows: model development. Biosyst. eng. 103, 105–115.

Huang, C., Wells, L.K., Norton, L.D., 1999. Sediment transport capacity and erosion processes: model concepts and reality. Earth Surf. Process. Landf. 24, 503–516.

Julien, P., Simons, D., 1985. Sediment transport capacity of overland flow. Trans. ASAE 28, 755–762.

Kainz, M., 1989. Runoff, erosion and sugar beet yields in conventional and mulched cultivation results of the 1988 experiment. Soil Technol. Ser. 1, 103–114.

Lal, R., 1998. Soil erosion impact on agronomic productivity and environment quality. Crit. Rev. Plant Sci. 17, 319–464.

Lang, R.D., 1990. The Effect of Ground Cover on Runoff and Erosion Plots at Scone, New South Wales. MSc Thesis. Macquarie University, Sydney.

Laufer, D., Loibl, B., Märländer, B., Koch, H.J., 2016. Soil erosion and surface runoff under strip tillage for sugar beet (*Beta vulgaris* L.) in Central Europe. Soil Tillage Res. 162 (1–7).

Lei, T.W., Zhang, Q., Zhao, J., Tang, Z., 2001. A laboratory study of sediment transport capacity in the dynamic process of rill erosion. Trans. ASAE 44, 1537.

Li, G., Abrahams, A.D., 1999. Controls of sediment transport capacity in laminar interrill flow on stone — covered surfaces. Water Resour. Res. 35, 305–310.

Liu, C., Luo, X., Liu, X., Yang, K., 2013. Modeling depth-averaged velocity and bed shear stress in compound channels with emergent and submerged vegetation. Adv. Water Resour. 60, 148–159.

Loch, R.J., 2000. Effects of vegetation cover on runoff and erosion under simulated rain and overland flow on a rehabilitated site on the Meandu Mine, Tarong, Queensland. Soil Res. 38, 299–312.

Mahmoodabadi, M., Ghadiri, H., Rose, C., Yu, B., Rafahi, H., Rouhipour, H., 2014a. Evaluation of GUEST and WEPP with a new approach for the determination of sediment transport capacity. J. Hydrol. 513, 413–421.

Mahmoodabadi, M., Ghadiri, H., Yu, B., Rose, C., 2014b. Morpho-dynamic quantification of flow-driven rill erosion parameters based on physical principles. J. Hydrol. 514, 328–336.

Martínez-Zavala, L., Jordán, A., 2008. Effect of rock fragment cover on interrill soil erosion from bare soils in Western Andalusia, Spain. Soil Use Manag. 24, 108–117.

Meyer, L., Wischmeier, W., 1969. Mathematical simulation of the process of soil erosion by water. Trans. ASAE 12, 754–758.

Moore, T.R., Thomas, D.B., Barber, R.G., 1979. The influence of grass cover on runoff and soil erosion from soils in the Machakos area, Kenya. Trop. Agrc. 56, 339–344.

Nanson, G.C., Beach, H.F., 1977. Forest succession and sedimentation on a Meandering-River Floodplain, Northeast British Columbia, Canada. J. Biochem. 4, 229–251.

Nearing, M.A., Foster, G.R., Lane, L.J., Finkner, S.C., 1989. A process-based soil Erosion model for USDA-water erosion prediction project technology. Trans. ASAE 32, 1587.

Noble, E., 1965. Sediment Reduction through Watershed Rehabilitation. U.S. Department of Agriculture, Washington, D.C.

Ouyang, W., Hao, F., Skidmore, A.K., Toxopeus, A.G., 2010. Soil erosion and sediment yield and their relationships with vegetation cover in upper stream of the Yellow River. Sci. Total Environ. 409, 396–403.

Pan, C.Z., Shangguan, Z.P., 2006. Runoff hydraulic characteristics and sediment generation in sloped grassplots under simulated rainfall conditions. J. Hydrol. 331, 178–185.

Pan, C.Z., Ma, L., Shangguan, Z.P., 2010. Effectiveness of grass strips in trapping suspended sediments from runoff. Earth Surf. Process. Landf. 35, 1006–1013.

Papy, F., Douyer, C., 1991. Influence des e'tats de surface du territoire agricole sur le de'clenchement des inondations catastrophiques. Agronomie 11, 201–215.

Prosser, I.P., Rustomji, P., 2000. Sediment transport capacity relations for overland flow. Prog. Phys. Geogr. 24, 179–193.

Rickson, R.J., Morgan, R.P.C., 1988. Approaches to modelling the effects of vegetation on soil erosion by water. In: Morgan, R.P.C., Rickson, R.J. (Eds.), Agriculture: Erosion Assessment and Modelling. Office for Official Publications of the European Communities, Luxembourg.

Rogers, R.D., Schumm, S.A., 1991. The effect of sparse vegetative cover on erosion and sediment yield. J. Hydrol. 123, 19–24.

Saltelli, A., Tarantola, S., Campolongo, F., Ratto, M., 2004. Sensitivity Analysis in Practice: A Guide to Assessing Scientific Models. Halsted Press, New York.

Shih, H.M., Yang, C.T., 2009. Estimating overland flow erosion capacity using unit stream power. Int. J. Sediment Res. 24, 46–62.

Silburn, D.M., Carroll, C., Ciesiolka, C.A.A., deVoil, R.C., Burger, P., 2011. Hillslope runoff and erosion on duplex soils in grazing lands in semi-arid central Queensland. I. Influences of cover, slope, and soil. Soil Res. 49, 105–117.

Snelder, D.J., Bryan, R.B., 1995. The use of rainfall simulation test to assess the influence of vegetation density on soil loss on degraded rangelands in the Baringo District, Kenya. Catena 25, 105–116.

Wischmeier, W.H., 1959. A rainfall erosion index for a universal soil-loss equation. Soil

Sci. Soc. Am. J. 23, 246–249.
Wu, S., Wu, P., Feng, H., Merkley, G.P., 2011. Effects of alfalfa coverage on runoff, erosion and hydraulic characteristics of overland flow on loess slope plots. Front. Env. Sci. Eng. 5, 76–83.
Wu, B., Wang, Z.L., Zhang, Q.W., Shen, N., Liu, J., Wang, S., 2018. Evaluation of shear stress and unit stream power to determine the sediment transport capacity of loess materials on different slopes. J. Soils Sediments 18, 116–127.
Yalin, M.S., 1963. An expression for bed-load transportation. J. Hydraul. Div. 89, 221–250.
Yu, B.F., Zhang, G.H., Fu, X.D., 2015. Transport capacity of overland flow with high sediment concentration. J. Hydrol. Eng. 20, C4014001.
Zhang, G.H., Liu, Y.M., Han, Y.F., Zhang, X.C., 2009. Sediment transport and soil detachment on steep slopes: I. transport capacity estimation. Soil Sci. Soc. Am. J. 73, 1291–1297.
Zhang, G.H., Liu, G.B., Wang, G.L., Wang, Y.X., 2011a. Effects of vegetation cover and rainfall intensity on sediment-bound nutrient loss, size composition and volume fractal dimension of sediment particles. Pedosphere 21, 676–684.
Zhang, G.H., Wang, L.L., Tang, K.M., Luo, R.T., Zhang, X.C., 2011b. Effects of sediment size on transport capacity of overland flow on steep slopes. Hydrol. Sci. J. 56, 1289–1299.
Zhang, J., Zhong, Y., Huai, W., 2018. Transverse distribution of streamwise velocity in open-channel flow with artificial emergent vegetation. Ecol. Eng. 110, 78–86.
Zhao, C.H., Gao, J.E., Huang, Y.F., Wang, G.Q., Zhang, M.J., 2016. Effects of vegetation stems on hydraulics of overland flow under varying water discharges. Land Degrad. Dev. 27, 748–757.
Zhou, Z.C., Shangguan, Z.P., Zhao, D., 2006. Modeling vegetation coverage and soil erosion in the Loess Plateau Area of China. Eco. Model. 198, 263–268.